molecular oral microbiology

molecular oral microbiology

Oral *Fusobacterium nucleatum* subsp. *polymorphum* binds to human salivary α-amylase

M. Zulfiqar, T. Yamaguchi, S. Sato and T. Oho

Department of Preventive Dentistry, Kagoshima University Graduate School of Medical and Dental Sciences, Kagoshima, Japan

Correspondence: Taihei Yamaguchi, Department of Preventive Dentistry, Kagoshima University Graduate School of Medical and Dental Sciences, 8-35-1 Sakuragaoka, Kagoshima 890-8544, Japan Tel./fax: + 81 99 275 6182; E-mail: yamatai@dent.kagoshima-u.ac.jp

Keywords: anaerobes; biofilms; oral microbiology; peridontal disease
Accepted 7 June 2013
DOI: 10.1111/omi.12036

SUMMARY

***Fusobacterium nucleatum* acts as an intermediate between early and late colonizers in the oral cavity. In this study, we showed that *F. nucleatum* subsp. *polymorphum* can bind to a salivary component with a molecular weight of approximately 110 kDa and identified the protein and another major factor of 55 kDa, as salivary α-amylase by time-of-flight mass spectrometry and immunoreactions. Salivary α-amylase is present in both monomeric and dimeric forms and we found that formation of the dimer depends on copper ions. The *F. nucleatum* adhered to both monomeric and dimeric salivary α-amylases, but the numbers of bacteria bound to the dimeric form were more than those bound to the monomeric form. The degree of adherence of *F. nucleatum* to four α-amylases from different sources was almost the same, however its binding to β-amylase was considerably decreased. Among four α-amylase inhibitors tested, acarbose and type 1 and 3 inhibitors derived from wheat flour showed significant activity against the adhesion of *F. nucleatum* to monomeric and dimeric amylases, however voglibose had little effect. Moreover *F. nucleatum* cells inhibited the enzymatic activity of salivary α-amylase in a dose-dependent manner. These results suggest that *F. nucleatum* plays more important and positive role as an early colonizer for maturation of oral microbial colonization.**

INTRODUCTION

Periodontal disease, one of the most common diseases, is highly prevalent all over the world. The disease is a chronic inflammatory disorder caused by multiple periodontopathic pathogens including *Fusobacterium nucleatum*, *Porphyromonas gingivalis*, and *Prevotella intermedia*. Moreover, periodontal disease has been associated with preterm birth, low birthweight, and threatened premature labor (Hasegawa *et al.*, 2003). The pathogens stimulate various types of cells including monocytes, chorion-derived cells and oral epithelial cells resulting in the production of bioactive mediators such as interleukin-1 (IL-1), IL-6, IL-8 and placental corticotrophin-releasing hormone (Kebschull & Papapanou, 2011; Tateishi *et al.*, 2012). Dental plaque is formed by streptococci, which act as early colonizers, on the acquired pellicles of teeth followed by late colonizers including periodontopathic pathogens. Matured plaque plays an important role in the progression of periodontal disease (Kolenbrander, 2000; Kolenbrander *et al.*, 2010). The control of plaque on the surface of teeth and in the subgingival pocket could be vital to prevent the disease.

The adherence of bacteria to host tissue is pivotal to the infection process. In the case of oral commensals, adhesion to the tooth surface is the first step in the formation of dental plaque (Socransky *et al.*,

1977). Associations between salivary components and bacteria play an important role in the adherence by providing adhesin-receptor structures and conversely, for clearance of the bacteria from the oral cavity by aggregation. Moreover, these salivary factors are associated with the development and maintenance of plaque (Douglas, 1994). These bacteria-binding proteins include amylase, cystatin, phosphoproteins, proline-rich proteins, and high-molecular-weight glycoproteins such as secretory immunoglobulin A (IgA), salivary agglutinin, and mucin bring about the adherence and aggregation of bacteria (Scannapieco, 1994). The secretion of each component differs in various salivary glands and this could result in different compositions of tooth surface pellicles formed in various parts of the dentition and mouth (Carlen *et al*., 1998).

Fusobacterium nucleatum is a Gram-negative anaerobe predominantly isolated in lesions of patients with gingivitis and chronic periodontitis (Moore & Moore, 1994; Teles *et al*., 2006). It coaggregates with various oral bacteria including *P. gingivalis*, *Treponema denticola* (Kolenbrander *et al*., 2002), *Capnocytophaga ochracea* (Okuda *et al*., 2012b), and *Prevotella* species (Okuda *et al*., 2012a), and is associated with the formation of a biofilm. Matured subgingival plaque could lead to periodontitis (Kolenbrander *et al*., 2010). Despite reports of coaggregation between early and late colonizers mediated by *F. nucleatum*, the *F. nucleatum* can attach to the surface of teeth directly through salivary components. The adhesion of all strains of *F. nucleatum* was enhanced by statherin-treated hydroxyapatite, but not hydroxyapatite treated with salivary proline-rich protein-1 (Xie et al., 1991). *F. nucleatum* is invasive and one of the species most frequently detected in amniotic fluid cultures from women with preterm labor and intact membranes (Han *et al*., 2004). Several kinds of periodontopathic bacteria including *F. nucleatum* have been isolated from carotid endarterectomy specimens of patients undergoing surgical treatment for atherosclerosis, and inflammation was suggested to be enhanced by the presence of the bacteria (Ford *et al*., 2006). Recently it was reported that *F. nucleatum* was isolated from chorionic tissues of high-risk pregnant women, but not normal pregnant women (Tateishi *et al*., 2012).

Although the coaggregation among oral bacteria has been well studied in relation the formation of oral biofilms, little is known about the effect of saliva. This study examines the correlation between salivary components and *F. nucleatum*, in an effort to find new ways to prevent *F. nucleatum* from attaching to tooth and mucosal surfaces, and to prevent infection of oral cavity and to arrest progression of systemic diseases.

MATERIALS AND METHODS

Bacteria and culture conditions

Fusobacterium nucleatum subsp. *polymorphum* (ATCC 10953) was grown in brain–heart infusion broth supplemented with 5 g l^{-1} yeast extract and 0.3 g l^{-1} cysteine-HCl at 37°C under anaerobic conditions using the AnaeroPack® Anaero system (Mitsubishi Gas Chemical Co., Inc., Tokyo, Japan). Following harvest at the late logarithmic phase, bacterial cells were washed three times with a phosphate buffer (pH 7.3) containing 2.7 mM KCl, 1.37 mM NaCl, 1.5 mM KH_2PO_4 and 2.7 mM Na_2HPO_4, and then suspended in it.

Collection of saliva and purification of salivary amylase

Whole saliva sample was collected by the spitting method from a healthy donor under stationary conditions. It was diluted twice with the phosphate buffer and supernatant was collected after centrifugation at 10,000 ***g*** for 15 min. Concentration of protein was determined with a Protein Assay Kit (Bio-Rad Laboratories, Hercules, CA) according to the instruction manual using bovine serum albumin as a standard. The clarified saliva (200 μg, 1 ml) was filtered through 0.2-μm membrane and applied to a column of Superdex 200 (GE Healthcare UK Ltd., Buckinghamshire, UK) equilibrated with 20 mM Tris–HCl (pH 6.8) and 0.15 M NaCl (TBS). The column was eluted at a flow rate of 0.5 ml min^{-1}, and fractions of 0.5 ml were collected. Each fraction was analyzed with sodium dodecyl sulfate–polyacrylamide gel electrophoresis (SDS–PAGE) and Western blotting.

SDS–PAGE and Western blotting

Electrophoresis was carried out in 1-mm thick 10% universal polyacrylamide slab gels equilibrated with Tris–glycine buffer. Before application, the samples

were heated with 2% SDS at 100°C for 3 min under non-reducing conditions unless otherwise stated. The gels were stained with a Rapid Stain CBB kit (Nacalai Tesque, Kyoto, Japan). For Western blotting, the proteins subjected to SDS–PAGE were electrophoretically transferred to polyvinylidene difluoride membranes. Immunoreactive proteins were visualized with anti-human amylase monoclonal immunoglobulins (Abnova, Taipei, Taiwan) and peroxidase-labeled anti-mouse IgG (Invitrogen, Calsbad, CA) followed by the ECL-Plus Western blotting detection system according to the manual provided (GE Healthcare).

Preparation of anti-*F. nucleatum* serum

Antiserum was generated using a pipetted extract derived from *F. nucleatum* ATCC 10953 as an antigen. Pathogen-free female BALB/c mice were purchased from Japan SLC (Hamamatsu, Japan). These mice were maintained in the experimental animal facility of Kagoshima University (Kagashima, Japan). All experiments were conducted in accordance with guidelines provided by the Kagoshima University Graduate School of Dentistry Animal Care Committee. Seven-week-old female mice were immunized subcutaneously three times at 2-week intervals and immunized serum was collected as described (Yamaguchi *et al.*, 2011).

Time-of-flight mass spectrometry (TOF-MS) analyses

The protein fraction was analyzed by SDS–PAGE and visualized using Coomassie Brilliant Blue R-250 stain. Each protein band was excised from the gel, and the gel pieces were destained with 25 mM NH_4HCO_3/50% acetonitrile [1 : 1 volume/volume (v/v)], dehydrated in acetonitrile, and dried in a vacuum evaporator. Cysteine residues in proteins were reduced with 10 mM dithiothreitol for 45 min at 56°C followed by alkylation with 50 mM iodoacetamide for 30 min at room temperature in the dark. The gel pieces were washed with 25 mM NH_4HCO_3/50% acetonitrile (1 : 1 v/v), dehydrated with acetonitrile, and dried using a vacuum evaporator. The proteins in gel were incubated with Trypsin Gold, Mass Spec Grade (Promega, Madison, WI) (5 μg ml^{-1}) in a digestion buffer (50 mM NH_4HCO_3) for 45 min on ice. After removal of the extra trypsin solution, the gel pieces were incubated in 50 μl of the digestion buffer for 24 h at 37°C. The peptides were extracted with 50% acetonitrile/5% trifluoroacetic acid, concentrated in a vacuum evaporator, and desalted using ziptip C-18. The samples were mixed with an equal volume of a saturated solution of α-cyano-4-hydroxycinnamic acid (Sigma-Aldrich, St Louis, MO) in 50% acetonitrile/0.1% trifluoroacetic acid. The peptides were analyzed by autoflex speed TOF/TOF-KG (Bruker Daltonics, Yokohama, Japan), and identified by a data base (the National Center for Biotechnology Information non-redundant protein database) search using the MASCOT software (Matrix Science, Tokyo, Japan).

Bacterial adsorption analyses

Clarified saliva sample was vigorously mixed with an equal volume of the phosphate buffer or *F. nucleatum* cell suspension (A_{600} = 10.0) for 10 min at room temperature followed by centrifugation at 15,000 ***g*** for 5 min. The supernatants containing proteins absorbed with the bacteria or non-absorbed proteins were simultaneously analyzed by SDS–PAGE and Western blotting for comparison.

Adherence assay of *F. nucleatum* to immobilized amylase

A solution (100 μl) containing an α-amylase derived from human saliva, *Bacillus* species (Sigma-Aldrich), *Bacillus licheniformis* (Sigma-Aldrich), or *Asperguillus oryzae* (Sigma-Aldrich), or a β-amylase from wheat seeds (MP Biomedicals, LLC, Solon, OH) in TBS was applied to microplate wells. The concentration of the amylase was 100 μg ml^{-1} unless otherwise stated. The plate was kept at 4°C overnight for immobilization. After blocking with TBS containing 0.2% Tween-20, 100 μl of *F. nucleatum* (A_{600} = 0.05) in TBS containing 1 mM $CaCl_2$ was added, centrifuged at 500 ***g*** for 10 min, and kept at room temperature for 30 min. The plate was washed three times with TBS containing 0.05% Tween-20 and 1 mM $CaCl_2$, and fixation was carried out with 200 μl of 3.7% formaldehyde. The plate was reacted with the anti-*F. nucleatum* serum followed by horseradish peroxidase-conjugated anti-mouse IgG. A color signal was developed by addition of *o*-phenylenediamine as a substrate. Absorbance at 450 nm was measured

every 5 min for up to 60 min in a microplate reader. Assays were performed in triplicate on three separate occasions. For the standard reaction, 100 μl aliquots of the *F. nucleatum* suspension (A_{600} = 0.05) and a series of diluted solutions were added to empty wells. After centrifugation, the supernatant was aspirated and cells on wells were dried out and fixed with formaldehyde. Cells were detected using the anti-*F. nucleatum* serum as above. The rate of binding was calculated and compared to the standard reaction. Absorbance derived from 100 μl of the cell suspension (A_{600} = 0.05) was defined as 100%.

The effect of α-amylase inhibitors on adherence of *F. nucleatum* to the salivary α-amylase was estimated. The *F. nucleatum* cells were suspended in TBS, 1 mM $CaCl_2$ containing 2 μg ml^{-1} inhibitor and absorbance at 600 nm was adjusted to 0.05. A solution (100 μl) of the bacterial suspension was added to wells coated with the salivary α-amylase. The inhibitors tested were voglibose, acarbose (Wako Pure Chemical Industries, Ltd., Osaka, Japan), and type 1 and 3 inhibitors derived from wheat flour (Sigma-Aldrich). Subsequent procedures were carried out as described above.

Iodostarch reaction

To assess the effect of the binding of *F. nucleatum* on the enzymatic activity of the amylase, an iodostarch reaction was carried out. Wells of a microplate were coated with 100 μl of 100 μg ml^{-1} salivary α-amylase solution overnight. An aliquot (100 μl) of diluted *F. nucleatum* suspension, whose absorbance at 600 nm ranged from 10 to 0, was added to wells, centrifuged and stood at room temperature for 30 min. After three washes with TBS containing 0.05% Tween-20, 50 μl of 0.5% starch solution was added and incubated at 37°C for 1 h followed by addition of 10 μl of 0.01% potassium iodide and 0.003% iodine. The plate was stood at room temperature for 10 min and absorbance at 450 nm was measured. The reaction with TBS instead of the *F. nucleatum* suspension was defined as 100% activity.

Statistical methods

The data were averaged (mean ± standard deviation) of the three independent experiments. Statistical analyses were performed by one-way analysis of variance (*post hoc* test: Dunnett) and *P*-values < 0.01 were considered significant.

RESULTS

Identification of salivary component associated with *F. nucleatum*

First we identified the salivary component that possessed affinity for *F. nucleatum* by conducting adsorption assay. Human saliva sample adsorbed with cells of *F. nucleatum* was subjected to SDS–PAGE (Fig. 1). When the adsorbed saliva was compared with the original saliva, a major band corresponding to a molecular weight of approximately 110 kDa, decreased considerably. To identify this interesting protein and another major salivary component with a molecular weight of 55 kDa, bands were excised and subjected to mass spectrometric analyses after in-gel trypsin digestion. Results showed both proteins to be salivary α-amylase. In Western blot analyses, both proteins reacted with the anti-amylase antibody (Fig. 1B). The 110-kDa protein was predominantly adsorbed with *F. nucleatum*.

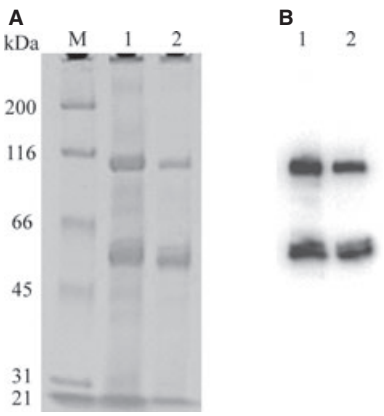

Figure 1 Identification of salivary component(s) with affinity for *Fusobacterium nucleatum*. (A) Saliva samples after adsorption with an equal volume of Tris-buffered saline (lane 1) or the *F. nucleatum* (ATCC 10953) cell suspension (OD_{600} = 10.0) (lane 2) were subjected to 10% sodium dodecyl sulfate–polyacrylamide gel electrophoresis (SDS–PAGE). The gel was stained with a Rapid Stain CBB kit. A portion of molecular mass standard was applied (lane M). (B) Saliva samples as in (A) were subjected to 10% SDS–PAGE and transferred to a polyvinylidene difluoride membrane. Salivary amylases were visualized using an anti-human amylase monoclonal antibody and chemi-luminescence substrate.

Purification of the α-amylase from human saliva

To purify the human salivary α-amylase, unstimulated saliva was subjected to Superdex 200 chromatography. The amylase was eluted in the third peak (Fig. 2A). Fractions 31–39 were subjected to 10% SDS–PAGE. Fractions 34–37 possessed a single protein of approximately 55 kDa (Fig. 2B). The distinct band was identified as an amylase by Western blotting (data not shown). The purified amylase was suggested to be monomeric. No dimeric amylase was detected in fractions 1 to 60. Fractions 34 to 37 were mixed and used as the purified salivary α-amylase in further examinations.

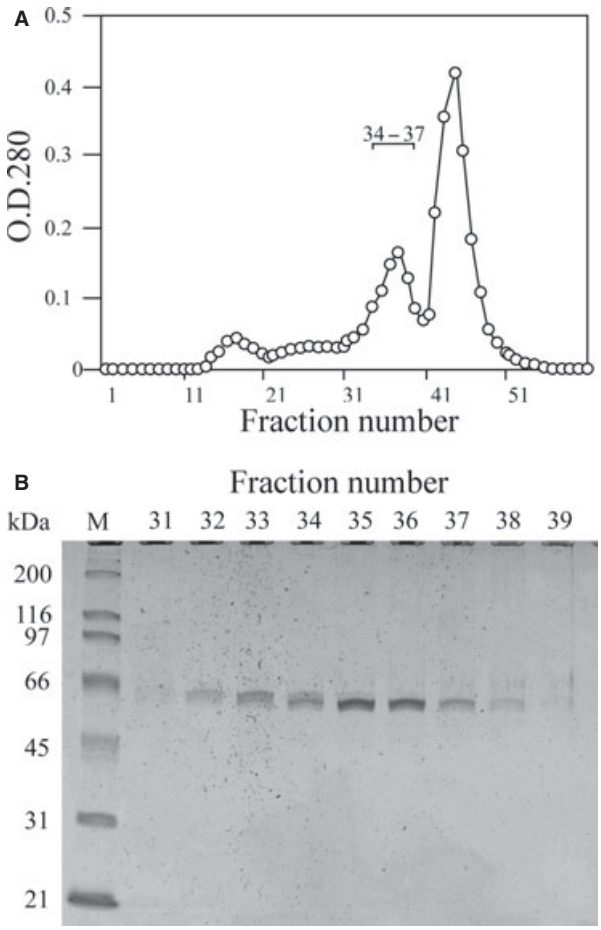

Figure 2 Purification of the α-amylase from human saliva. (A) The clarified saliva was fractionated by Superdex 200 column chromatography (1.5 × 30 cm) as described in the Materials and methods. Fractions 34–37 were mixed and used as the purified material for further analyses. (B) Sodium dodecyl sulfate–polyacrylamide gel electrophoresis (SDS–PAGE) of each fraction (10 μl) from the gel filtration. Numbers in each lane are the fraction number. Specimens were heated at 100°C for 3 min under non-reducing conditions. A portion of the molecular mass standard was applied also (lane M).

Formation of the dimeric form of human salivary α-amylase

We estimated various conditions for forming a dimeric amylase. The purified salivary amylase (1.6 μg) was incubated in the presence of 1 mM of various metal ions and subjected to SDS–PAGE (Fig. 3A). Only copper sulfate brought about production of the dimeric form. Copper chloride demonstrated the same effect as copper sulfate. The amylase self-aggregated and was trapped on the bottom of wells in the presence of iron (III) sulfate. No other tested metal ions except for copper and iron (III) ions affected the formation of the dimer, and there was only the monomeric form. When the pH was changed (from 4 to 8) or the concentration of NaCl was changed (from 0 to 1 M), no dimeric molecules were formed (data not shown).

To assess the molecular interaction between the amylase and copper, different concentrations of copper ion were evaluated (Fig. 3B). The CBB-stained band of the dimeric form thickened gradually in a dose-dependent manner. In contrast, the monomeric form decreased with an increase in copper sulfate, and little was detected at 10 mM of copper sulfate. Under reducing conditions, the dimer was readily separated to monomeric molecules regardless of copper ion (Fig. 3C).

Adherence of *F. nucleatum* to immobilized human salivary α-amylase

To characterize the adherence of *F. nucleatum* to amylase, purified α-amylase was coated on the surface of a microplate. When adherence to the dimeric α-amylase was examined, α-amylase in the buffer containing 10 mM copper sulfate was used. The adhered bacteria were measured by immunoreaction, and per cent adherence was determined by comparing bacteria applied (Fig. 4). When 100 μl of 100 μg ml^{-1} α-amylase was used, approximately 18% of bacteria adhered to the monomeric form, and approximately 40% more *F. nucleatum* cells adhered to the dimeric than monomeric α-amylase. These results indicate that formation of the dimer of salivary a-amylase is predominantly associated with binding to *F. nucleatum*.

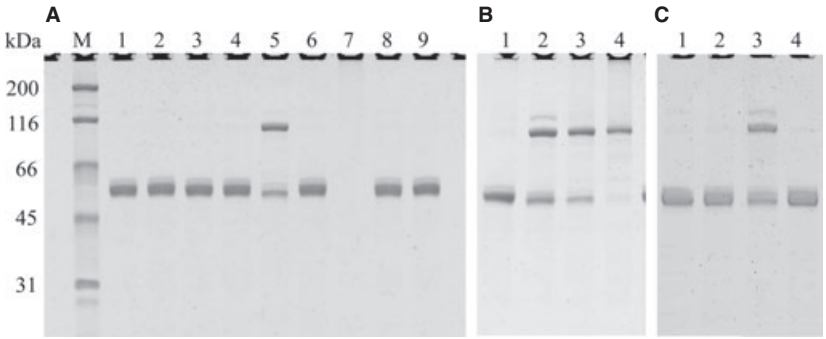

Figure 3 Effect of metal ions on the formation of dimeric molecules of the salivary α-amylase. (A) The purified α-amylase was incubated in the presence of 1 mM of metal ions, which were Tris-buffered saline (lane 1), $CaCl_2$ (lane 2), $MgCl_2$ (lane 3), $MnCl_2$ (lane 4), $CuSO_4$ (lane5), $NiCl_2$ (lane 6), $Fe_2(SO_4)_3$ (lane 7), $ZnSO_4$ (lane 8), and EDTA (lane 9). These samples were heated at 100°C for 3 min under non-reducing conditions and subjected to sodium dodecyl sulfate–polyacrylamide gel electrophoresis (SDS-PAGE). A portion of the molecular mass standard was applied also (lane M). (B) The purified α-amylase was incubated in the presence of several concentrations of $CuSO_4$. The concentrations were 0 mM (lane 1), 0.1 mM (lane 2), 1.0 mM (lane 3) and 10.0 mM (lane 4). These samples were analyzed by SDS–PAGE as in (A). (C) The purified α-amylase was incubated in the absence (lanes 1 and 2) or with 0.1 mM (lanes 3 and 4) of $CuSO_4$. These samples were mixed with an equal volume of sample buffer containing 4% SDS (lanes 1 and 3) and additional 10% β-mercaptoethanol (lanes 2 and 4). After heat treatment, analyses by SDS–PAGE were performed as in (A).

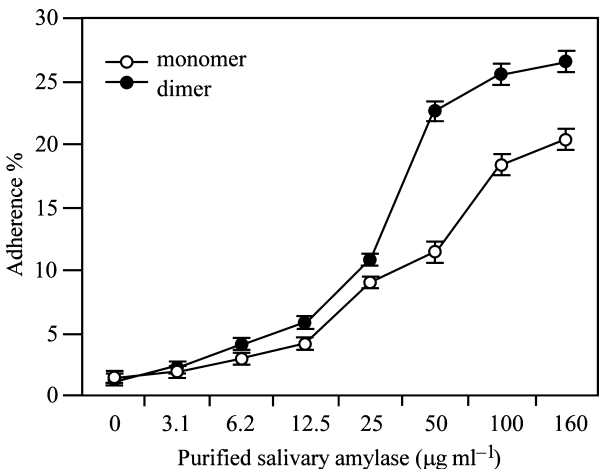

Figure 4 Adherence of *Fusobacterium nucleatum* to the salivary α-amylase immobilized on micro wells. Various amounts of the salivary α-amylase were added to micro wells in the absence of copper ion for the monomeric form or in the presence of 10 mM copper sulfate for the dimeric form, and incubated at 4°C overnight. After washing and blocking, *F. nucleatum* (A_{600} = 0.05) was added. The plate was centrifuged and left at room temperature for 30 min. The wells were washed and fixed, and numbers of bacteria adhered were measured using an immunoreaction with anti-*F. nucleatum* cell antiserum. Values are indicated as a percentage of the number of bacteria applied. All assays were performed in triplicate on three separate occasions. Data are expressed as means ± standard deviations.

Adherence of *F. nucleatum* to some amylases

To examine whether the adherence of *F. nucleatum* is specific to the human salivary α-amylase, we used three other α-amylases and a β-amylase. *F. nucleatum* adhered to all the α-amylases tested to a similar degree, but its adherence to β-amylase was considerably reduced (Fig. 5). The adherence to β-amylase was <30% of that to monomeric human α-salivary amylase. These results suggest that the common structure of α-amylases plays an important role in binding of *F. nucleatum* to each amylase in comparison with β-amylase.

Inhibition of the adherence of *F. nucleatum* by α-amylase inhibitors

Several inhibitors of α-amylase have been reported, including both carbohydrates and proteinaceous molecules. It is important for resolving the mechanism of interaction between amylases and *F. nucleatum* to clarify whether the catalytic structure of amylases is associated with the adherence. Exogenous voglibose, a monosaccharide, weakly inhibited the adherence of *F. nucleatum* to the monomeric amylase (Fig. 6A). On the other hand, acarbose, a pseudo-tetrasaccharide, brought about significant inhibition. Two proteinaceous inhibitors derived from wheat flour demonstrated considerable inhibitory activity, with type 3 inhibitor being slightly more effective than the type 1 inhibitor. These results indicate that *F. nucleatum* recognizes the catalytic structure of the α-salivary amylase. The effect of the same inhibitors on dimeric amylase was estimated

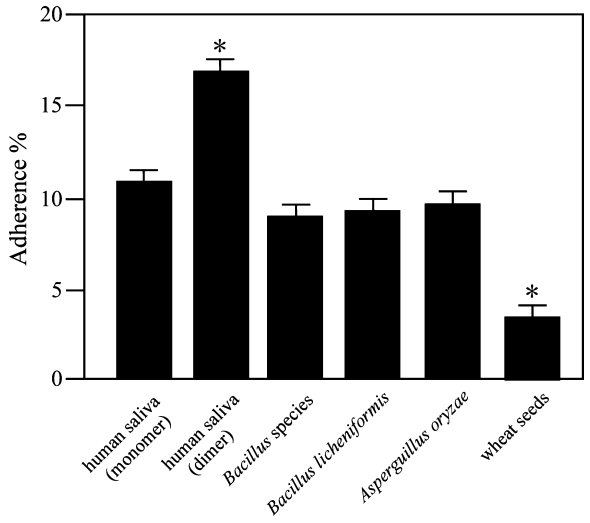

Figure 5 Adherence of *Fusobacterium nucleatum* to amylases derived from various sources. An aliquot of amylase (100 μg ml^{-1}, 100 μl) was coated on a 96-well micro plate and kept at 4°C overnight. Amylases used were human salivary α-amylase, α-amylases from *Bacillus* species, *Bacillus licheniformis*, *Aspergillus oryzae* and a β-amylase from wheat seeds. The salivary α-amylase was added to wells in the presence of 10 mM $CuSO_4$ in order to form a dimeric molecule. After washing and blocking, *F. nucleatum* (A_{600} = 0.05) was added. The plate was centrifuged and kept at room temperature for 30 min. The wells were washed and fixed, and numbers of bacteria adhered to amylase were measured by an immunoreaction with anti-*F. nucleatum* cell antiserum. Values are indicated as a percentage of the number of bacteria applied. All assays were performed in triplicate on three separate occasions. Data are expressed as means ± standard deviations. Asterisks indicate significant differences ($P < 0.01$) from the control value (adherence to human salivary α-amylase: monomeric form).

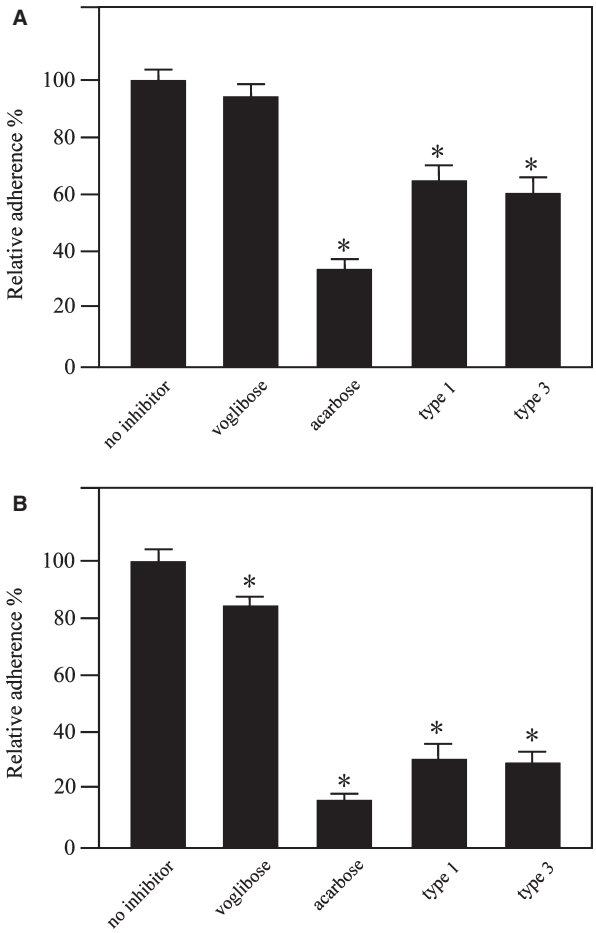

Figure 6 Inhibitory effect of α-amylase inhibitors on the binding of *Fusobacterium nucleatum* to immobilized salivary α-amylase. The inhibitors used were voglibose, acarbose, and type 1 and 3 inhibitors derived from wheat flour. The *F. nucleatum* cells were incubated in plastic wells coated with monomeric amylase (A) or dimeric amylase (B) in the presence of 2 μg ml^{-1} of inhibitor. Values are indicated as a percentage of the number of bacteria adhered to the amylase under conditions without an inhibitor. All assays were performed in triplicate on three separate occasions. Data are expressed as means ± standard deviations. Asterisks indicate significant differences ($P < 0.01$) from the control value (without inhibitor).

also. A similar tendency as for the monomeric amylase was observed (Fig. 6B). However, the reduction of adherence by all inhibitors tested was higher than in the case of the monomeric amylase.

Inhibition of enzymatic activity of salivary α-amylase by binding of *F. nucleatum*

To determine the site where the human α-amylase binds to *F. nucleatum* more directly, the enzymatic activity of amylase, which was pretreated with *F. nucleatum* cells, was evaluated (Fig. 7). When the immobilized amylase was preincubated with *F. nucleatum*, the activity decreased gradually depending on the number of bacterial cells applied. Eventually, the activity reached almost zero. A similar effect was obtained using the dimeric amylase as a coating agent. Although the inhibitory effect indicated almost the same tendency under both conditions, the activity of dimeric amylase was a little lower than monomeric amylase when high numbers of bacteria were added.

DISCUSSION

Amylase is a major secretory proteinaceous component of human saliva. It has significant biological functions, most important is the initial digestion of starch, glycogen and other polysaccharides in the oral cavity. However, amylase coated on teeth acts

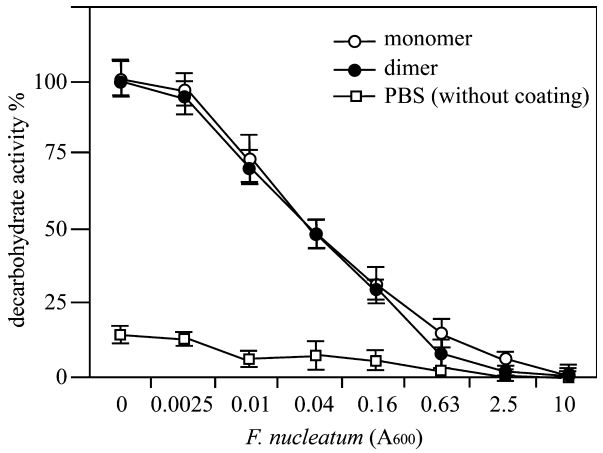

Figure 7 Inhibitory effect of *Fusobacterium nucleatum* on α-amylase activity. Increasing numbers of *F. nucleatum* cells were incubated in plastic wells coated with monomeric amylase, dimeric amylase or phosphate-buffered saline (PBS). After centrifugation and incubation for 30 min followed by a wash to remove unbound cells, a starch solution was added and kept for 1 h. Values are percentages of the activity of the amylase when no *F. nucleatum* cells were present. All assays were performed in triplicate on three separate occasions. Data are expressed as means ± standard deviations.

as a foothold for the proliferation of oral commensals. Amylase binds specifically and with high affinity to a number of oral streptococcal species, which are classified as early colonizers in the human oral cavity. (Douglas, 1983; Kilian & Nyvad, 1990). These findings suggest that the ability to bind to amylase plays an important role in oral colonization by streptococci and brings about an ecological advantage. *Fusobacterium nucleatum* coaggregates with both early and late colonizers on the surface of teeth. Almost none of the late colonizers coaggregate with each other. The *F. nucleatum* places itself at the border between early and late colonizers (Kolenbrander *et al.*, 2002). The present study demonstrated that *F. nucleatum* can adhere to not only statherin but also to human salivary amylase. On the other hand, *P. gingivalis* is a gram-negative anaerobe closely associated with periodontitis and acts as a late colonizer (Griffen *et al.*, 1998). It has been reported that *P. gingivalis* coaggregates with various oral bacteria including actinomyces, streptococci, prevotella, treponema and fusobacteria. The characteristics are suggested to contribute to the colonization of *P. gingivalis* with early colonizers (Sato & Nakazawa, 2012). Moreover, high-resolution analyses using mass spectrometry indicated that lipopolysaccharides of *P. gingivalis* bound to several salivary components as well as α-amylase (Choi *et al.*, 2011). These results suggested that *F. nucleatum* as well as *P. gingivalis* has an ability to adhere to teeth coated with salivary components directly and also function as early colonizers.

Amylases catalyze the hydrolysis of α-1,4-glucosidic linkages of starch and glycogen to produce oligosaccharides in the α-anomeric configuration (MacGregor *et al.*, 2001). Some α-amylases form a dimeric structure. *Thermoactinomyces vulgaris* R-47 α-amylase, a TVA II enzyme, has a domain N located before the N-terminal of domain A. Experiments with a domain N truncated mutant demonstrated that the domain plays an important role in the formation of dimer and for enzymatic activity. In contrast, TVA I enzyme cannot form a dimeric structure in spite of possessing domain N, and the ability to recognize various substrates is different from that of TVA II (Yokota *et al.*, 2001). The dimerization of glycosyltrehalose trehalohydrolase from *Sulfolobus solfataricus* was based on a different mechanism. Although this enzyme has a typical domain N, a set of molecules was covalently linked by an intermolecular disulfide bond located outside of domain N (Feese *et al.*, 2000). Human salivary α-amylase is composed of domains A, B and C and does not have a domain N. The structure of human salivary amylase was determined and the ultimate structure of a non-crystallographic symmetric dimer was demonstrated in space group C2. The interface between the monomers was a complex interdigitation of loops, creating a large amount of buried surface area between the dimer interface (approximately 2800 $Å^2$). In comparison with the monomer, the dimeric form has little conformational change in domain A (Fisher *et al.*, 2006). Here we described that formation of the dimer was achieved with copper ions and the linkage between the monomers was resistant to heat treatment in the presence of SDS. In contrast, the dimer was easily broken down to monomers under reducing conditions. These results suggest that this mechanism of dimerization is specific to salivary α-amylase and different from TVA II and glycosyltrehalose trehalohydrolase.

As described above, the catalytic structure, which is located in domain A, is not considerably different from monomeric and dimeric human salivary amylases, and each catalytic site derived from paired amylases in dimer is located separately. This indicates that the specificity and affinity for substrate

could be almost the same or very similar to each other. Acarbose was least-squares fitted independently onto each monomeric molecule of the dimer, and both of the fitted acarboses exhibited no steric clashes within the active sites of the monomers (Qian *et al*., 1994). Instead, the enzymatic activity of dimeric human salivary amylase was approximately 30% higher than that of monomer molecule in the iodo-starch reaction (data not shown), and in this study we observed that more *F. nucleatum* cells adhered to dimeric molecule than to monomeric molecule. Because dimer formation in the presence of copper ions is reported in this study for the first time, considerable conformational change in the catalytic area may happen by those copper ions. Such change by dimer formation could affect the bacterial binding as well as the enzymatic activity.

In this study we assessed the effect of four α-amylase inhibitors on the binding of *F. nucleatum*. Each inhibitor had a specific effect on the activity of human salivary α-amylase. Among the inhibitors tested, acarbose displayed tremendous inhibitory activity. However, voglibose, which is a simple sugar, possessed weak inhibitory activity. This difference could be due to the affinity of these compounds for the specific structural domain of the salivary amylase recognized by *F. nucleatum*. These characteristics were almost consistent with the inhibition of glycosidase activity on the digestion of starch (Ren *et al*., 2011). The results suggested that *F. nucleatum* interacted with the catalytic cleft of the amylase. Type 1 and 3 inhibitors from wheat flour (*Triticum aestivum*) had a specific inhibitory effect on α-amylases derived from different sources (O'Connor & McGeeney, 1981). Amount of type 1 inhibitor needed for almost complete inhibition of human salivary α-amylase was 12 times more than type 3 inhibitor. Both inhibitors demonstrated 50–95% inhibition for human pancreatic amylase in comparison with salivary amylase. In contrast, no effect on α-amylase from germinated wheat was detected using any of the inhibitors. Here we evaluated the inhibitory activity of types 1 and 3 on adherence of *F. nucleatum* to salivary α-amylase and certainly both molecules demonstrated a similar significant effect. Moreover, *F. nucleatum* cells inhibited the enzymatic activity of salivary α-amylase in a dose-dependent manner. Inhibitory effect of *F. nucleatum* to immobilized dimeric amylase was a little stronger than to monomeric amylase when high numbers of bacteria were added. It may be hard to see differences under these conditions with the assay system used in this study.

All of these results suggest that binding of *F. nucleatum* interacts with the decarbohydrate catalytic area of α-amylase directly or indirectly. However, the detailed mechanism for the binding is still unclear. Identification of the bacterial factor could provide significant information for clarifying the association between the bacteria and α-amylase in more detail, and it could define the role of fusobacteria on the formation and maturation of dental plaque.

ACKNOWLEDGEMENTS

We thank Dr Yuichi Oogai and Professor Hitoshi Komatsuzawa, Department of Oral Microbiology, Kagoshima University Graduate School of Medical and Dental Sciences for help with the TOF-MS analyses. We are also indebted to Takeshi Nishiyama, Department of Preventive Dentistry, Kagoshima University Graduate School of Medical and Dental Sciences for the statistical analyses. This study was supported in part by Grants-in-aid for Scientific Research (C) 23593093 (T.Y.) and Challenging Exploratory Research 23659987 (T.O.) from the Japan Society for the Promotion of Science.

REFERENCES

Carlen, A., Borjesson, A-C., Nikdel, K. and Olsson, J. (1998) Composition of pellicles formed *in vivo* on the tooth surfaces in different parts of the dentition, and *in vitro* on hydroxyapatite. *Caries Res* **32**: 447–455.

Choi, S., Baik, J.E., Jeon, J.H. *et al.* (2011) Identification of *Porphyromonas gingivalis* lipopolysaccharide-binding proteins in human saliva. *Mol Immunol* **48**: 2207–2213.

Douglas, C.W.I. (1983) The binding of human salivary alpha-amylae by oral strains of streptococcal bacteria. *Arch Oral Biol* **28**: 567–573.

Douglas, C.W.I. (1994) Bacterial–protein interactions in the oral cavity. *Adv Dent Res* **8**: 254–262.

Feese, M.D., Kato, Y., Tamada, T. *et al.* (2000) Crystal structure of glycosyltrehalose trehalohydrolase from the hyperthermophilic archaeum *Sulfolobus solfataricus*. *J Mol Biol* **301**: 451–464.

Fisher, S.Z., Govindasamy, L., Tu, C. *et al.* (2006) Structure of human salivary α-amylase crystallized in a C-centered monoclinic space group. *Acta Cryst* **62**: 88–93.

Ford, P.J., Gemmell, E., Chan, A. *et al.* (2006) Inflammation, heat shock proteins and periodontal pathogens in atherosclerosis: an immunohistologic study. *Oral Microbiol Immunol* **21**: 206–211.

Griffen, A.L., Becker, M.R., Lyons, S.R., Moeschberger, M.L. and Leys, E.J. (1998) Prevalence of *Porphyromonas gingivalis* and periodontal health status. *J Clin Microbiol* **36**: 3239–3242.

Han, Y.W., Redline, R.W., Li, M., Yin, L., Hill, G.B. and McCormick, T.S. (2004) *Fusobacterium nucleatum* induces premature and term stillbirths in pregnant mice: implication of oral bacteria in preterm birth. *Infect Immun* **72**: 2272–2279.

Hasegawa, K., Furuichi, Y., Shimotsu, A. *et al.* (2003) Association between systemic status, periodontal status, serum cytokine levels, and delivery outcomes in pregnant women with a diagnosis of threatened premature labor. *J Periodontol* **74**: 1764–1770.

Kebschull, M. and Papapanou, P.N. (2011) Periodontal microbial complexes associated with specific cell and tissue responses. *J Clin Periodontol* **38**: 17–27.

Kilian, M. and Nyvad, B. (1990) Ability to bind salivary alpha-amylase discriminates certain viridans group streptococcal species. *J Clin Microbiol* **28**: 2576–2577.

Kolenbrander, P.E. (2000) Oral microbiol communities: biofilms, interactions, and genetic systems. *Annu Rev Microbiol* **54**: 413–437.

Kolenbrander, P.E., Andersen, R.N., Blehert, D.S., Egland, P.G., Foster, J.S. and Palmer, R.J. Jr (2002) Communication among oral bacteria. *Microbiol Mol Biol Rev* **66**: 486–505.

Kolenbrander, P.E., Palmer, R.J., Periasamy, S. and Jakubovics, N.S. (2010) Oral multispecies biofilm development and the key role of cell–cell distance. *Nat Rev Microbiol* **8**: 471–480.

MacGregor, E.A., Janeček, Š. and Svensson, B. (2001) Relationship of sequence and structure to specificity in the α-amylase family of enzymes. *Biochem Biophys Acta* **1546**: 1–20.

Moore, W.E. and Moore, L.V. (1994) The bacteria of periodontal diseases. *Periodontology* **5**: 66–77.

O'Connor, C.M. and McGeeney, K.F. (1981) Isolation and characterization of four inhibitors from wheat flour which display differential inhibition specificities for human salivary and human pancreatic α-amylases. *Biochim Biophys Acta* **658**: 387–396.

Okuda, T., Kokubu, E., Kawana, T., Saito, A., Okuda, K. and Ishihara, K. (2012a) Synergy in biofilm formation between *Fusobacterium nucleatum* and *Prevotella* species. *Anaerobe* **18**: 110–116.

Okuda, T., Okuda, K., Kokubu, E., Kawana, T., Saito, A. and Ishihara, K. (2012b) Synergistic effect on biofilm formation between *Fusobacterium nucleatum* and *Caonocytophaga ochracea*. *Anaerobe* **18**: 157–161.

Qian, M., Haser, R., Buisson, G., Duee, E. and Payan, F. (1994) The active center of a mammalian alpha-amylase. Structure of the complex of a pancreatic alpha-amylase with a carbohydrate inhibitor refined to 2.2-A resolution. *Biochemistry* **33**: 6284–6294.

Ren, L., Cao, X., Geng, P., Bai, F. and Bai, G. (2011) Study of the inhibition of two human maltase-glucoamylases catalytic domains by different α-glucosidase inhibitors. *Carbohydrate Res* **346**: 2688–2692.

Sato, T. and Nakazawa, F. (2012) Coaggregation between *Prevotella oris* and *Porphyromonas gingivalis*. *J Microbiol Immunol Infect* doi:10.1016/j.jmii.2012.09.005.

Scannapieco, F.A. (1994) Saliva-bacterium interactions in oral microbial ecology. *Crit Rev Oral Biol Med* **5**: 203–248.

Socransky, S.S., Manganiello, A.D., Propas, D., Oram, V. and van Houte, J. (1977) Bacteriological studies of developing supragingival dental plaque. *J Periodontal Res* **12**: 90–106.

Tateishi, F., Hasegawa-Nakamura, K., Oogai, T. *et al.* (2012) Detection of *Fusobacterium nucleatum* in chorionic tissues of high-risk pregnant women. *J Clin Periodontol* **39**: 417–424.

Teles, R.P., Haffajee, A.D. and Socransky, S.S. (2006) Microbiological goals of periodontal therapy. *Periodontology* **42**: 180–218.

Xie, H., Gibbons, R.J. and Hay, D.I. (1991) Adhesive properties of strains of *Fusobacterium nucleatum* of the subspecies nucleatum, vincentii and polymorphum. *Oral Microbiol Immunol* **6**: 257–263.

Yamaguchi, T., Soutome, S. and Oho, T. (2011) Identification and characterization of a fibronectin-binding protein from *Granulicatella adiacens*. *Mol Oral Microbiol* **26**: 353–364.

Yokota, T., Tonozuka, T., Kamitori, S. and Sakano, Y. (2001) The deletion of amino-terminal domain in *Thermoactinomyces vulgaris* R-47 α-amylase: effects of domain N on activity, specificity, stability and dimerization. *Biosci Biotechnol Biochem* **65**: 401–408.